私立東海大學

資訊工程與科學研究所

碩士論文

指導教授：黃育仁 教授

3-D 乳房超音波影像區域成長乳房腫瘤輪廓描繪

Three-dimensional region growing segmentation for breast tumor on sonography

研究生：張順展

中 華 民 國 九 十 九 年 七 月

摘要

乳癌是現今婦女最常見罹患的癌症，其乳癌致死人數往往在各國十大癌症死因排行中佔居前三名，但隨著醫療技術的不斷進步，乳癌致死率可以因患者早期發現早期治療而降低致死率，醫學診斷乳房腫瘤良惡性的方法中又以超音波影像具有非侵入式、即時造影及費用便宜等優點，因此為目前最普遍使用的診斷方式，目前現行的醫學診斷方式需依賴醫師豐富的臨床經驗，透過超音波影像中腫瘤的輪廓、大小、形狀分析腫瘤良惡性，但超音波影像中經常包含大量的雜訊及紋理特徵，容易影響醫師正確判讀結果，在診斷上可能會因為醫師的經驗不足而造成誤判影響到後續的病情控制，因此如果自動描繪的乳房腫瘤輪廓能夠與醫師手動描繪的腫瘤輪廓極為相似，將有助於提升醫師診斷腫瘤良惡性的正確率，在本研究中將提出乳房超音波影像腫瘤輪廓描繪方法，首先需先透過影像前處理去除超音波影像雜訊並強化影像對比度，使後續做腫瘤輪廓切割具有較高的準確率，腫瘤輪廓切割方法採用 3D region growing 方法描繪出腫瘤輪廓，最後再透過腫瘤輪廓後處理階段分析陰影在超音波影像中具有的特性，將 3D region growing 所描繪的腫瘤輪廓中包含腫瘤陰影的區域移除，在本研究中使用 20 個 case 進行實驗，分別為 10 個良性 case，10 個惡性 case，經過實驗結果顯示利用所提出的腫瘤輪廓切割方法，能夠與醫師手動描繪的腫瘤輪廓極為相似。

關鍵字：乳癌、超音波影像、影像切割、3D 區域成長、腫瘤輪廓切割

ABSTRACT

Breast malignant and benign tumor exist discrepancy in shape and size on sonography, information about shape and size provided by tumor's contour is important in clinical diagnosis. Due to ultrasound image includes noises and tissue texture, clinical diagnosis must be highly depends on expertise experience. However, manually sketch the three-dimensional (3D) breast tumor contour is a time-consuming and complicated task. Automatic contouring which provided the similar contour with manual sketch of the breast tumor in the ultrasonic images might assist physicians in making a correct diagnosis. This study presents an efficient method for automatically detecting 3D contours of breast tumors in sonography. The proposed method performs voxel nearest neighbor (VNN), Wiener filter and unsharp filter to enhance contrast and reduce noise. The 3D region growing algorithm is utilized to obtain the contour of breast tumor and then contour post-processing analyzes the extracted contour to diminish the shadow region of tumor. This study evaluates total of 20 tumor cases, comprising 10 benign and 10 malignant cases. The results of computer simulation reveal that the proposed 3D segmentation method provides a robust contouring for breast US image. This approach always identifies similar contours as that obtained by manual contouring of the breast tumor and could save much of the time required to sketch precise contours.

Keywords: breast cancer, sonography, image segmentation, 3D region growing, tumor contour approximation

INDEX

LIST OF TABLES

LIST OF FIGURES

CHAPTER1

INTRODUCTION

Breast cancer has become the second lead cause of cancer death among women not only in the United States of American but also all over the world. The death rate from breast cancer for woman is getting higher. However, breast cancer death rates have been going down in current year. It is probably the result of finding the cancer early and better diagnostic breast tumor technical. Ultrasound imaging and mammography are two main modalities for clinical diagnosis of breast cancer. Ultrasound has been popular medical imaging technique due to ultrasound imaging has the advantage of providing non-invasive, real time, relatively inexpensive and safe. Moreover, breast malignant and benign tumor exist discrepancy in shape and size on sonography, information from the tumor contours is important to make diagnostic decision. Due to ultrasound image always includes noises and tissue texture, clinical diagnosis must be highly depends on expertise experience. Manually sketch the three-dimensional (3D) breast tumor contour is very time-consuming and complicated task for inexperienced and young radiologist. For this purpose, automatic contouring which provided the similar contour with manual sketch of the breast tumor in the ultrasonic images might assist physicians in making correct diagnoses.

Three-dimensional (3D) ultrasound image has been a popular medical imaging

technique due to the entire volume of the breast tumor in the 3D ultrasound image can be obtained and freedom of view, relative to the two-dimensional (2D) ultrasound imaging. Some correct diagnostic decisions required entire volume information of the tumor and tumor contour. Conventional 2D ultrasound image consist of thin slices of the patient, expert must mentally build the impression of 3D tumor by many 2D ultrasound images. Moreover, malignant and benign breast tumor exist discrepancy in volume, the volume data of breast tumor [1-3] has been considered as a useful characteristic for identify malignant breast tumor.

Many approaches for ultrasound segmentation have been investigated, such as region-based image segmentation methods [4-6] or clustering-based image segmentation methods [7-9]. Region-based image segmentation methods attempt to partition or group region according to image properties. Morphological watershed segmentation is a popular region-based segmentation method, which always provides closed contours and requires low computation times in comparison with other segmentation methods. Morphological watershed segmentation is useful in ultrasound image segmentation, but conventional morphological watershed transformation are sensitive to the noise, that would cause over-segmentation due to ultrasound images always include lot of noise and tissue texture and then obtain unsatisfied contours. Clustering-based image segmentation methods are regarded as a process of

minimization of the intensity distance between every pixel and cluster center. Neural network segmentation method, one of the clustering-based segmentation methods, has a sample structure for physical implementation and can easily map complex distributions. Unfortunately, the method of image segmentation partition or group area without using spatial information, disconnected area of the image are grouped together and training sample required. Thus neural network segmentation method does not perform well for detecting contour of tumor in ultrasound image. In order to solve the problems, this study used 3D region growing method as the principal segmentation process in ultrasound image. Region growing segmentation partition or group area using spatial information, disconnected area of the image were not grouped to together and can performs well with respect to noise. The concept is simple and only need a small number of seed point to grow the desired region.

The aim of this paper was to develop a practical segmentation scheme for 3D breast ultrasound imaging. The propose segmentation method consisted three phases, i.e. image preprocessing, image segmentation and contour post-processing. The image preprocessing phase performed voxel nearest neighbor (VNN) [10;11], Wiener filter [12] and unsharp filter [13;14] to enhance contrast of breast tumor images and reduce noises, which suppressed the effect of noise on the accuracy of the segmentation result and improved accuracy of segmentation substantially. The image segmentation

phase sketched breast tumor contour by using the 3D region growing techniques. However the proposed region growing method might not distinguish the undesired shadow area of tumor due to the shadow area and tumor tissue held similar intensity. The contour post-processing phase analyzed the extracted contour to diminish the shadow area of tumor. Twenty patients were applied on the proposed 3D segmentation method. This study evaluated the automatic contouring results of breast tumor contours with manual sketch from experienced expert. The results of computer simulation reveal that the proposed 3D segmentation method always achieved a reliable performance.

CHAPTER2

MATERIALS AND METHODS

2.1 DATA ACQUISITION

The image database utilized in this study was collected during the period of July 2007 to August 2009, there were 10 benign and 10 malignant breast tumors in 20 patients whose ages ranged from 17 to 80 years (mean age, 44 years). Sonographic examinations were done by using 3D power Doppler ultrasound with the HDF function (Voluson 730, GE Medical Systems, Zipf, Austria). A linear-array broadband probe with a frequency of 6–12 MHz, a scan width of 37.5 mm, and a sweep angle of 5° to 29° to obtain 3D volume scanning was used. Expert kept a fixed sweep angle of 20° and power Doppler settings of mid frequency, 0.9 kHz pulse repetition frequency, −0.6 gain, and 'low 1' wall motion filter in all cases. All obtained images were stored on the hard disk and transferred to a personal computer using a DICOM (Digital Imaging and Communications in Medicine) connection for image analysis. Each 3D imaging contained approximately 200 2D slices, the spatial resolution of each slice was approximately 250 × 100 pixels. The entire database was supplied by the co-author an experienced breast surgeon, D-RC from the Comprehensive Breast Cancer Center, Changhua Christian Hospital, Changhua, Taiwan. D-RC is a breast surgeon.

2.2 MANUAL CONTOURING

An experienced sonography physician who was familiar with breast ultrasound interpretations manually determined 3D contours of the tumor by using two distinct modes. The entire manual sketching (EMS) mode denoted physician manually sketched 2D contour on each slice of a tumor. The partial manual sketching (PMS) mode denoted the virtual organ computer-aided analysis (VOCAL) [15-17] scheme within 4D View software (GE Medical Systems, Zipf, Austria) was performed to obtain an approximated 3D contour. Then the obtained contours were saved in files for comparison with the automatically generated contours. The VOCAL scheme estimates 3D contours by a selectable degree of rotation. This study adopted a very common rotation degree 30^{o}, the six preliminary tumor contours in 0°, 30°, 60°, 90°, 120° and 150° slice images were manually sketched. Figure 1 represents the tumor contour manually sketched with 30° rotation. The PMS mode utilized the six extracted tumor regions to build a 3D interested region volume.

Moreover, this study developed an automatic version of the PMS mode, denoted partial automatic sketching (PAS) mode. In the PAS mode, six preliminary tumor contours extracted by using 2D region growing method were instead of the manually sketched contours. Physician was only required to select an initial seed point inside a breast tumor on the 0° slice of 3D sonography. The 2D region growing procedure

began from the defined seed point and estimated contours for each 30° rotation.

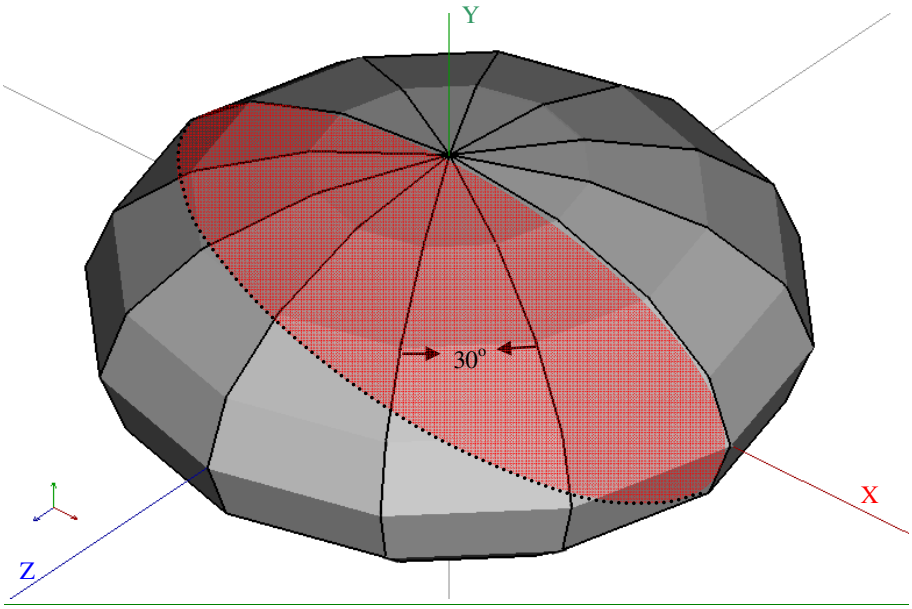

Fig. 1. The tumor contour that manually sketched with 30° by export

2.3 IMAGE PREPROCESSING

Figure 2 presents a flowchart of the proposed method, in a form that includes the image preprocessing, image segmentation and contour post-processing. Preprocessing is a significant step before the segmentation due to breast ultrasound images always including noises, speckles and tissue textures that make contour segmentation difficult. This study combined voxel nearest neighbor (VNN) algorithm, Wiener filtering and unsharp filtering to reduce noise and enhance image contrast. The VNN algorithm, a statistical based approach, consists of two steps. The first step was to determine whether or not a voxel was locating in a homogeneous region. Let $N_{26}(v)$ denoted local 26-adjacency [18;19] around a 3D voxel v.

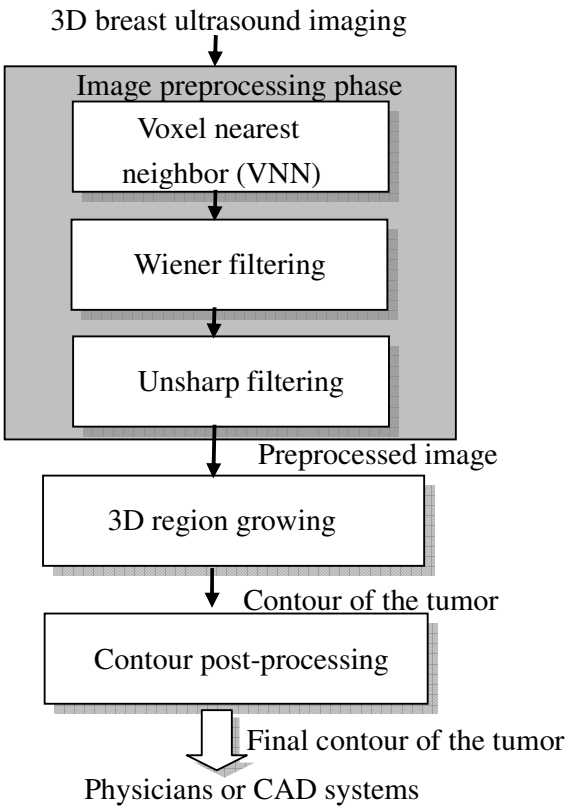

Fig. 2. The flowchart of the proposed method

Figure 3 shows the neighbors of a voxel within 26-adjacency. This study evaluated the number of voxel below a predefined threshold in $N_{26}(v)$. If the vast majority of voxel in $N_{26}(v)$ below the VNN threshold T_v, the voxel was considered as locating in a homogeneous region, otherwise the voxel was considered as locating in an inhomogeneous region. The second step of VNN algorithm was calculated and assigned the new value for voxels in homogeneous/inhomogeneous region. If a voxel was locating in homogeneous region, the method utilized a 3D mean filter to reduce noise. Contrarily, if the voxel was locating in inhomogeneous region, the new value v_n for the voxel was applied as

$$v_n = e^{(\sigma/\mu)} \times b \times v_i \,, \tag{1}$$

where σ and μ are the standard deviation and mean in $N_{26}(v)$, v_i is i^{th} voxel in the set $N_{26}(v)$ and b is a constant parameter controlling the rate of enhancement contrast. Figure 4(b) illustrates an example obtained by using the VNN algorithm. This study also utilized Wiener filtering and unsharp filtering to reduce noise and preserve detail information. Wiener filtering is popular and widely used filter, which reduce amount of noise. However, Wiener filtering not only smooths ultrasound images but also might remove detail information. Thus the unsharp filtering was performed after the Wiener filtering. Unsharp filtering improves the contour detail by removing low-frequency spatial information from the result of Wiener smoothing. After preprocessing of the ultrasound images, this study extracted precise contour of breast tumor based on the following segmentation steps. Figure 4(c) represents the result of the proposed image preprocessing procedure.

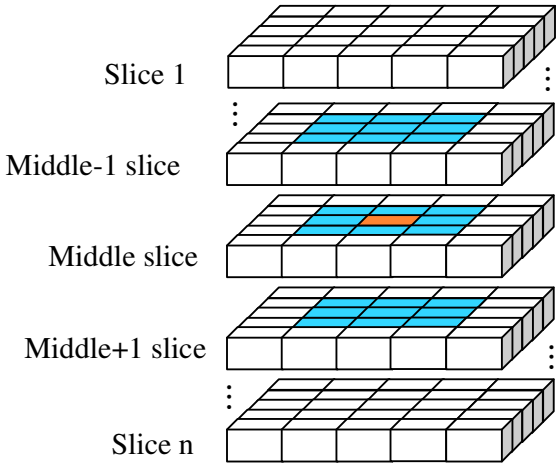

Fig. 3. Neighbors (the blue voxels) within the 26-connectivity

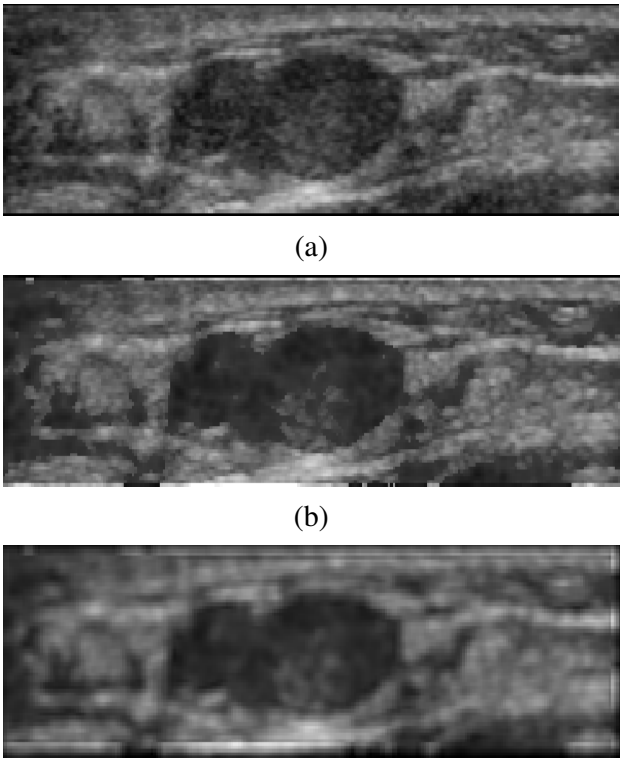

(a)

(b)

(c)

Fig. 4. Result of image preprocessing: (a) the original tumor image, (b) the enhanced result by using the VNN algorithm and (c) the final preprocessed image of the proposed method

2.4 IMAGE SEGMENTATION

To extract the volume of interest (VOI) in 3D ultrasound imaging, a physician with experience in breast ultrasound examination defined and manually selected rectangular region of interest (ROI) including the tumor border in the specific three slices, i.e. the first, middle and last slices in 3D ultrasound imaging [20]. The first, middle, and last slices were the slice with appeared tumor, the largest diameter of the tumor and the tumor is tending to disappear, respectively. The ROI is specified by

indicating a rectangular box that delimits the scene domain and describing the single target in a volume space constructs a VOI. After the ROI regions in the three slices were defined, the VOI area would be extracted from the 3D volume. Figure 5 presents the ROI data maps into VOI area.

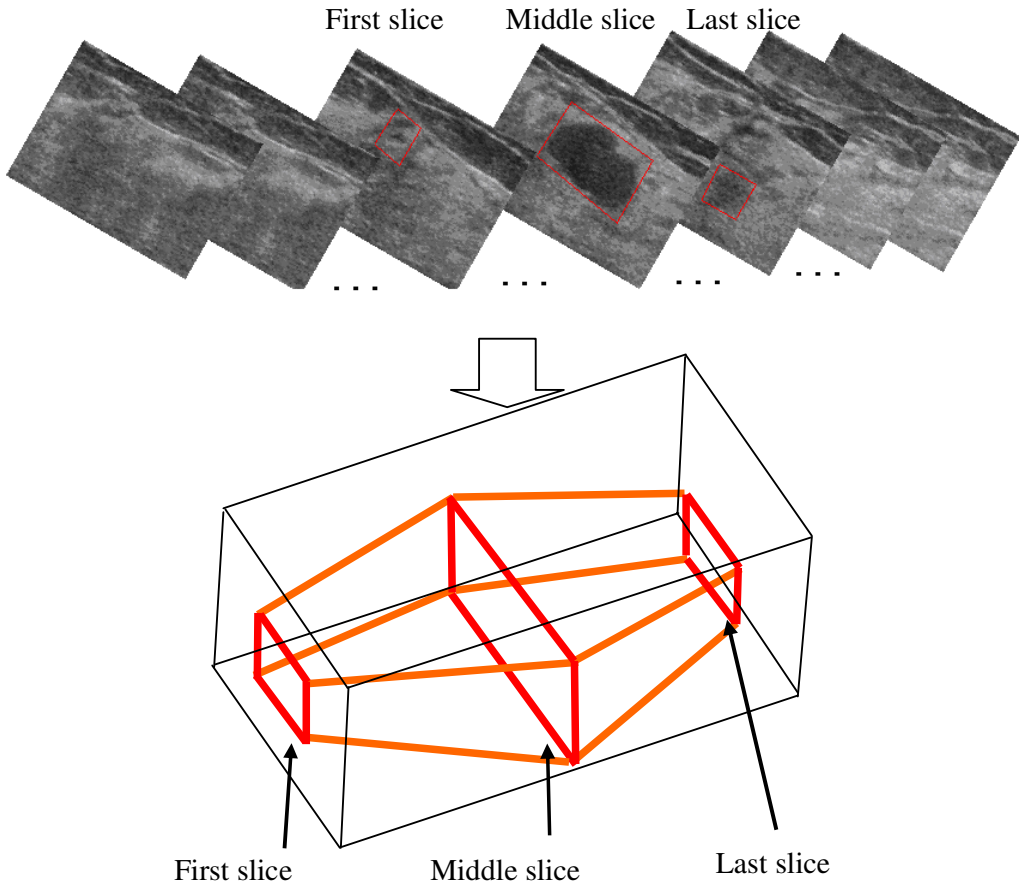

Fig. 5. The volume of interest (VOI) area in a 3D ultrasound imaging

Region growing technique is a useful, simple, and sophisticated method for image segmentation. Basically, the concept of 2D and 3D region growing are identical. The procedure starts with a set of seed points and groups neighboring voxels or subregions that provided similar properties into to larger regions. This study

performed the automatic 3D region growing method to separate the tumor region from background. Due to the largest diameter of the tumor always appears in middle slice of 3D sonography, the proposed method chose the centroid of ROI area in middle slice as the initial seed point. The intensity property to be used to include a voxel in either region is that the absolute difference of intensity between a voxel and the seed point be less that a predefined property threshold T_p. In this study, the mean intensity of tumor region was re-calculated. Any adjacent voxel that satisfies the intensity property for the subregion was assigned into tumor region. The entire procedure was repeated until no further changes occur. Figures 6 illustrate the result of 3D region growing procedure.

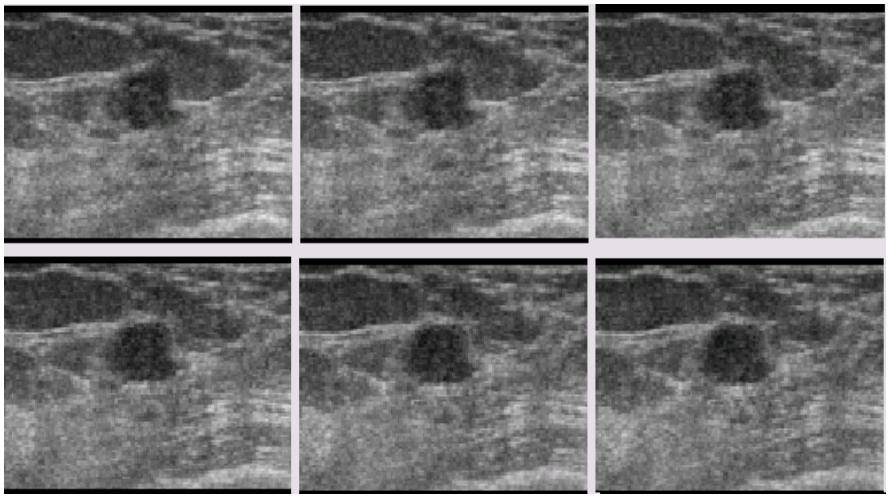

(a)

Fig. 6. Results of 3D region growing contour segmentation: (a) the original tumor image, (b) the result of EMS mode, (c) by the proposed segmentation method (continued)

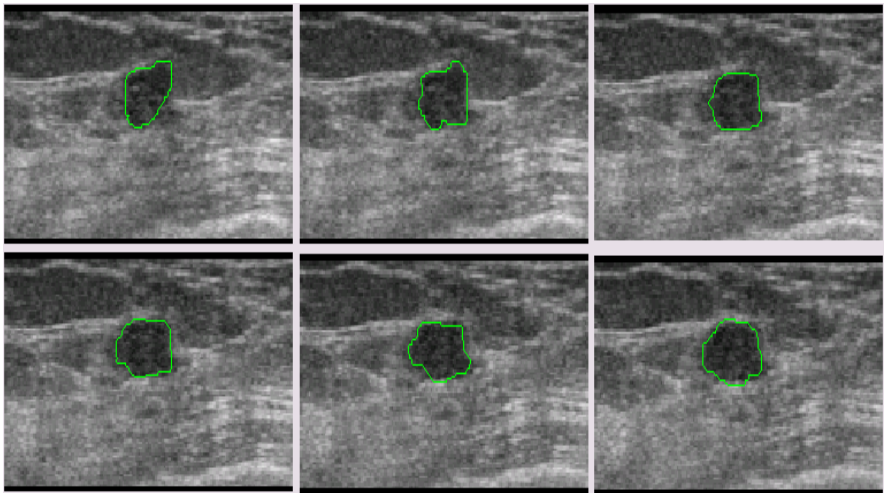

(b)

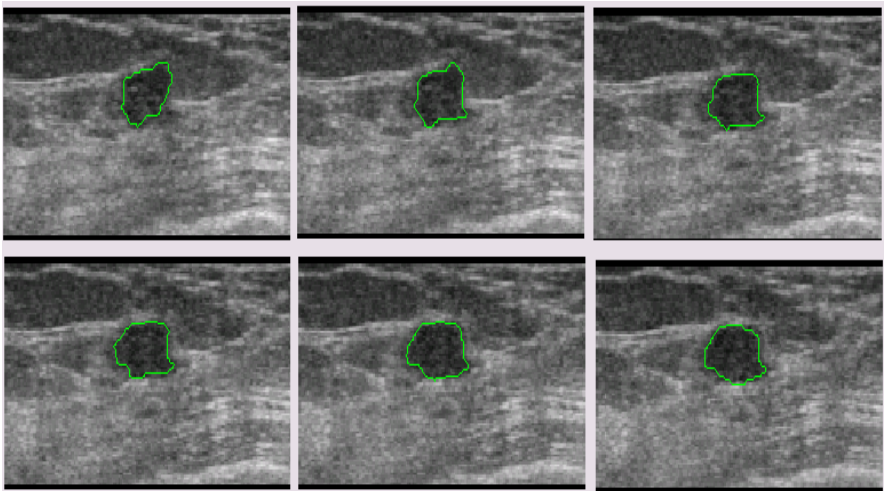

(c)

Fig. 6. Results of 3D region growing contour segmentation: (a) the original tumor image, (b) the result of EMS mode, (c) by the proposed segmentation method

2.5 CONTOUR POST-PROCESSING

The region growing procedure might not identify the shadow area in the tumor region due to the tissue portion and shadow portion in tumor region possesses a similar intensity sometimes. Thus contour post-processing step was in need to eliminate the shadow area and retain the true tumor region. The shadows of tumor had

specific properties by observing the contour of breast tumor, such as shadows of tumor always occur below the tumor and were slender in shape. Therefore, the proposed post-processing method analyzed the height of extracted contour of tumor that ranged from 70% and detected suspicious shadow area. Let two predefined thresholds T_r and T_c denotes the maximum of row width ratio and the minimum of column height ratio, respectively. The definition of the suspicious shadow area is that the width for each row of extracted tumor contour is lower than T_r and the height for column of suspicious shadow region is larger that T_c. Figures 7 show the result of the proposed post-processing procedure.

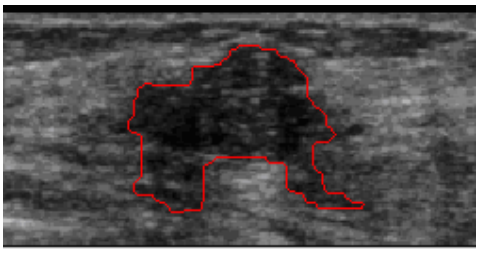

(a)

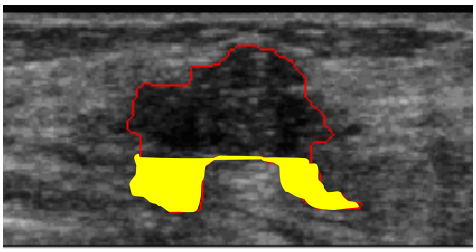

(b)

Fig. 7. Result of the contour post-processing: (a) the original contour in tumor, (b) to analyze the height of extracted contour of tumor that from 70%, (c) result of the post-processed contour (green contour) (continued)

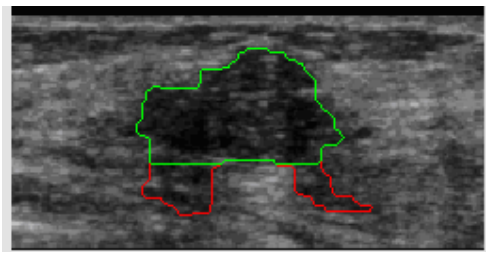

(c)

Fig. 7. Result of the contour post-processing: (a) the original contour in tumor, (b) to analyze the height of extracted contour of tumor that from 70%, (c) result of the post-processed contour (green contour)

2.6 CONTOUR EVALUATION

The accuracy of segmentation was measured by two metrics, similarity measures and performance measures. In similarity measures, four similarity measures [21], the similarity index (*SI*), overlap fraction (*OF*), overlap value (*OV*), and extra fraction (*EF*) between the manually sketched contours and the automatically determined contours were calculated for quantitative analysis of the contouring result. The *SI* is defined as

$$SI = \frac{2 * (REF \bigcap SEG)}{REF + SEG}, \tag{2}$$

where *REF* and *SEG* denote the areas covered by the manually sketched contours (by an experienced physician) and that covered by the contours generated by the proposed system, respectively. Figure 8 illustrates the relationship between the *REF* and *SEG*. The *overlap* denotes the area of the intersection of the reference and the automated

segmentation. The *SI* expresses the similar degree between *SEG* and *REF* areas. The *OF*, *OV* and *EF* are defined as

$$OF = \frac{REF \cap SEG}{REF}, \tag{3}$$

$$OV = \frac{REF \cap SEG}{REF \cup SEG}, \tag{4}$$

$$EF = \frac{\overline{REF} \cap SEG}{REF}, \tag{5}$$

The *OF* and *OV* measure the correctly segmented area relative to the reference area. The *EF* measures the area that is falsely segmented as lesion relative to the area in the reference. When *SI*, *OF* and *OV* are close to 1, and *EF* is close to 0, it means that the contour determined by the proposed segmentation is similar to manually sketched contours.

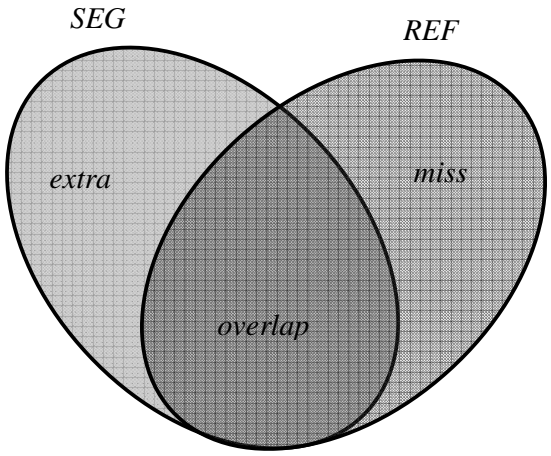

Fig. 8. The relationship between the tumor contour extracted by proposed segmentation algorithm (*SEG*) and the tumor contour manually sketched by expert (*REF*), *overlap* area denotes the correctly segmented pixels, *extra* area denotes the false positive area and *miss* area denote false negatives area

In the performance measures, the true positive (TP), false positive (FP), false negative (FN), true negative (TN), sensitivity and accuracy, were used to estimate the performance of the proposed system. The TP denotes the number of correct segmented region. FP denotes the number of incorrect segmentation region. FN denotes the number of region selected by manual segmentation but not by automatic contouring. TN denotes the region excluded from the segmentation common to both the automatic and manual segmentation. The sensitivity of segmentation can be defined as

$$Sensitivity = \frac{TP}{TP + FN}, \tag{6}$$

and represent the percentage of voxels that truly belong to the tumor region which were correctly identified as such. Also, accuracy is defined as

$$Accuracy = \frac{TP + TN}{TP + TN + FP + FN}, \tag{7}$$

When the results of contour segmentation are done precisely, the sensitivity and accuracy are close to 1.

CHAPTER3

EXPERIMENTAL RESULT

This approach compared the segmentation results among the proposed segmentation method, PMS and PAS modes. A total of 20 pathology proved tumor cases, comprising 10 benign tumors (numbered 1 to 10) and 10 malignant tumors (numbered 11 to 20) were enrolled in the study. In this work, the image preprocessing was first performed to reduce noise and preserve detail information. The VNN method set threshold T_v as 0.25 experimentally and the rate of enhancement contrast b was 0.9. And then image segmentation procedure employed 3D region growing method with the threshold T_p as 0.045 to extract contour of breast tumor. In contour post-processing, the thresholds T_r and T_c were set at 32.2% and 7.2% to diminish the shadow region of tumor, respectively.

Table 1 illustrates the result of not include contour post-processing and contour post-processing. The indices on not include contour post-processing were 0.82 for *SI*, 0.92 for *OF*, 0.70 for *OV* and 0.32 for *EF*. The indices on contour post-processing were 0.90 for *SI*, 0.88 for *OF*, 0.81 for *OV* and 0.08 for *EF*. Figures 9 show the result applied the proposed segmentation method, EMS, PMS and PAS on benign tumors. Figures 10 illustrate the segmentation results from malignant cases. Figures 11 show the measures of segmentation result with *SI*, *OF*, *OV*, *EF* and volume ratio. The

volume ratio is the proportion of the extracted tumor volume to that of physician manually sketched (EMS mode). The average indices of measure (*SI*, *OF*, *OV*, *EF*) on tumor contours from the proposed segmentation method, PMS, PAS modes are (0.94, 0.94, 0.89, 0.06), (0.80, 0.84, 0.67, 0.29) and (0.79, 0.75, 0.65, 0.15), respectively. Tables 2-5 illustrate the assessment indices among the three modes. The performance measures such as sensitivity and accuracy are calculated for the proposed segmentation method and are presented in Table 6. The average sensitivity was 0.942 and the average accuracy was 0.996. The simulations were made on a single CPU Intel Q9400 personal computer with Microsoft Windows XP® operating system and the program development environment was MATLAB (R2008.a) software (The MathWorks, Inc., Natick, MA).

Table 1. The result of not include contour post-processing and contour post-processing

Pathology proven result	*SI*	*OF*	*OV*	*EF*
Not include contour post-processing	0.823	0.922	0.700	0.320
Contour post-processing	0.90	0.884	0818	0.08

SI: similarity index; *OF*: overlap fraction; *OV:* overlap value; *EF*: extra fraction

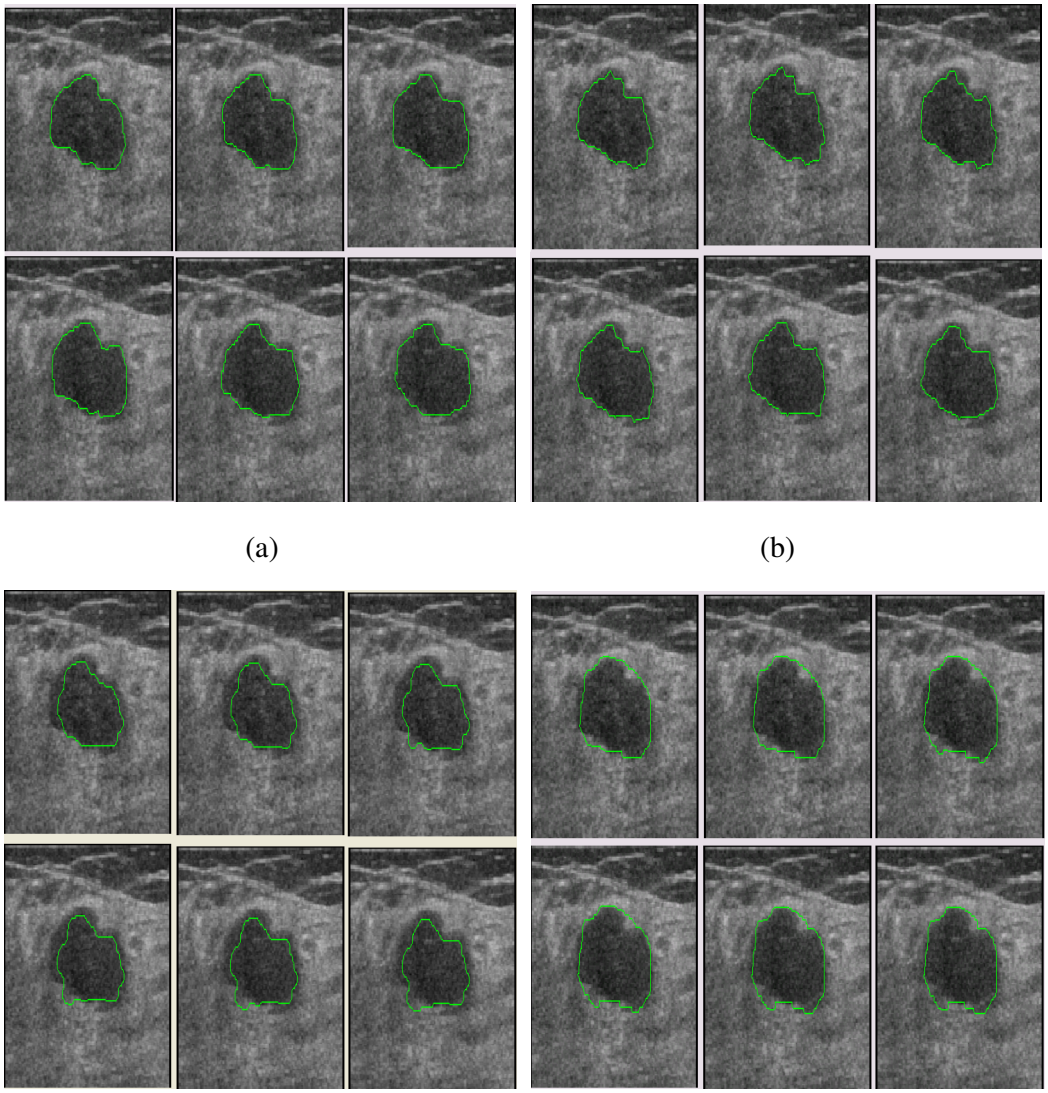

(a) (b)

(c) (d)

Fig. 9. Results of contour segmentation (benign case): (a) contours created manually by EMS mode, (b) through with the proposed segmentation method, (c) through with PAS mode, and (d) through with PMS mode

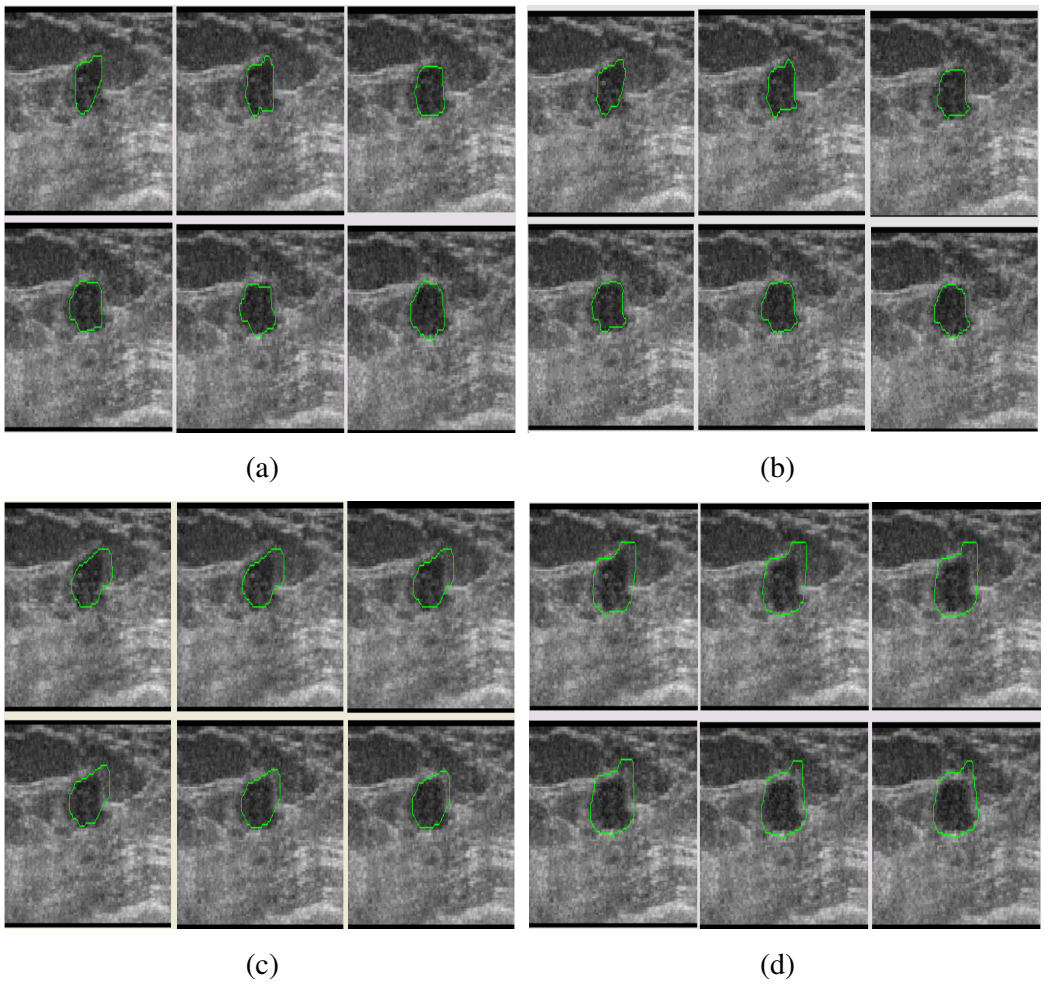

(a) (b)

(c) (d)

Fig. 10. Results of contour segmentation (malignant case) tumors: (a) contours created manually by EMS mode, (b) through with the proposed segmentation method, (c) through with PAS mode, and (d) through with PMS mode

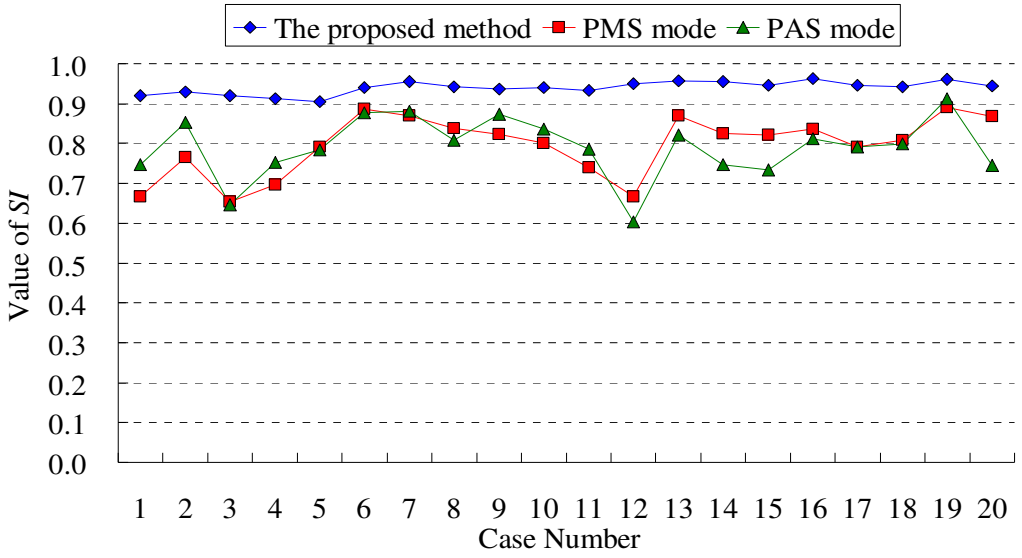

(a)

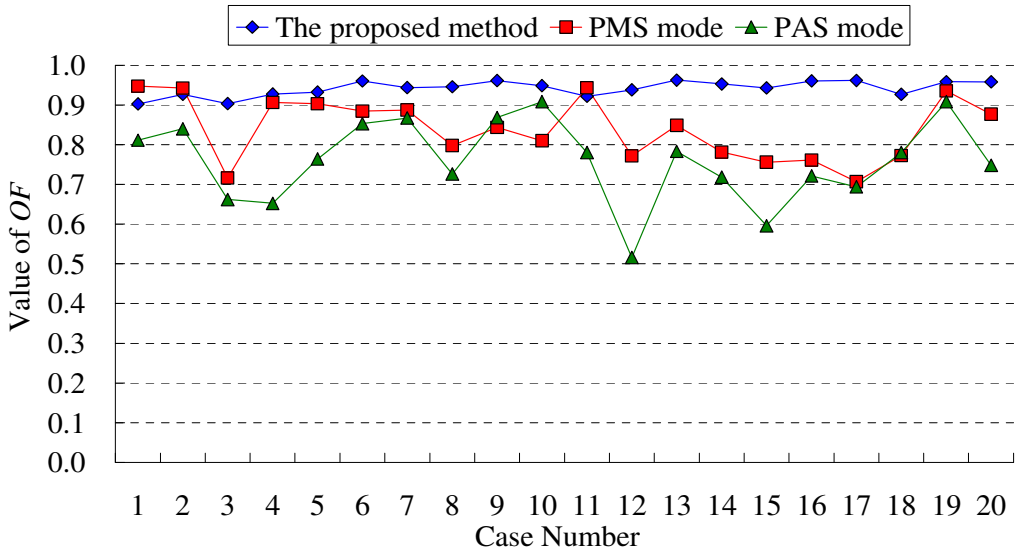

(b)

Fig. 11. Comparisons of contouring performance: (a) similarity index (*SI*), (b) overlap fraction (*OF*), (c) overlap value (*OV*), (d) extra fraction (*EF*) and (e) volume ratio (continued)

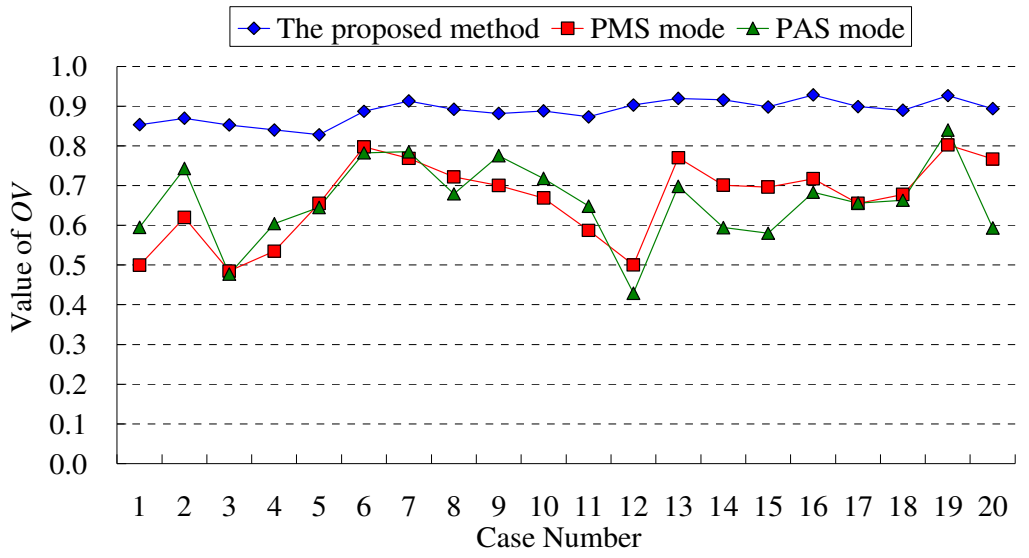

(c)

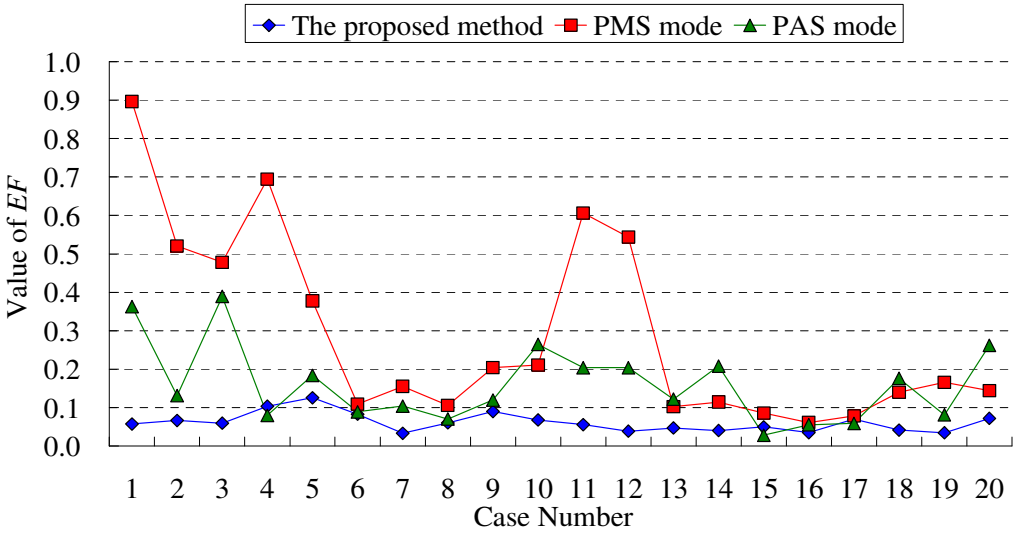

(d)

Fig. 11. Comparisons of contouring performance: (a) similarity index (*SI*), (b) overlap fraction (*OF*), (c) overlap value (*OV*), (d) extra fraction (*EF*) and (e) volume ratio (continued)

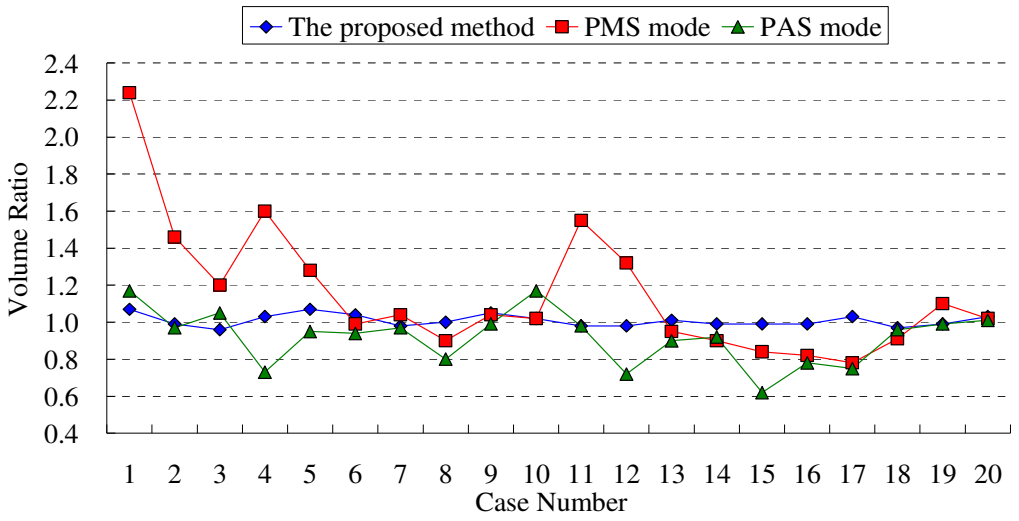

(e)

Fig. 11. Comparisons of contouring performance: (a) similarity index (*SI*), (b) overlap fraction (*OF*), (c) overlap value (*OV*), (d) extra fraction (*EF*) and (e) volume ratio

Table 2. The contouring evaluations using similarity index (*SI*) for US images

Pathology proven result	Average *SI*		
	The proposed segmentation method	PMS mode	PAS mode
Benignancy (10 cases)	0.931	0.779	0.806
Malignance (10 cases)	0.950	0.811	0.775
Whole database (20 cases)	0.940	0.795	0.790

Table 3. The contouring evaluations using overlap fraction (*OF*) for US images

Pathology proven result	Average *OF*		
	The proposed segmentation method	PMS mode	PAS mode
Benignancy (10 cases)	0.935	0.864	0.795
Malignance (10 cases)	0.948	0.815	0.724
Whole database (20 cases)	0.942	0.839	0.760

Table 4. The contouring evaluations using overlap value (*OV*) for US images

Pathology proven result	Average *OV*		
	The proposed segmentation method	PMS mode	PAS mode
Benignancy (10 cases)	0.870	0.645	0.680
Malignance (10 cases)	0.905	0.687	0.638
Whole database (20 cases)	0.887	0.666	0.659

Table 5. The contouring evaluations using extra fraction (*EF*) for US images

Pathology proven result	Average *EF*		
	The proposed segmentation method	PMS mode	PAS mode
Benignancy (10 cases)	0.075	0.375	0.179
Malignance (10 cases)	0.049	0.204	0.140
Whole database (20 cases)	0.062	0.290	0.160

Table 6. Performance measures of the proposed segmentation method of breast tumor

Pathology proven result	Sensitivity	Accuracy
Benignancy (10 cases)	0.936	0.997
Malignance (10 cases)	0.948	0.996
Whole database (20 cases)	0.942	0.996

Sensitivity= TP / (TP+FN);

Accuracy= (TP+TN) / (TP+TN+FP+FN)

CHAPTER4

CONCLUSION

Superficial measure and shape information from tumor's contours can be used in clinical diagnosis. Shape based ultrasound imaging diagnosis of breast tumor takes the advantage of nearly independent to the different machines. However, it relies on physicians to manually segment tumors. A physician couldn't manually sketch the contours of tumors in a 3D sonography of many hundreds of two-dimension images. This study proposed an efficient method for detecting contours of breast tumor in 3D sonography. In the PMS and PAS modes, the six preliminary tumors contours were created by physician and 2D region growing method, respectively. Physician manually depict the six preliminary tumor contours or give an initial seed point for extract contour of tumor in breast ultrasound imaging. The procedure was faster and save much of the time required to sketch tumor. However, the PMS and PAS modes didn't perform well for detecting contour of tumor. That is because by using the preliminary six tumor contours to build 3D breast tumor, result of the tumor contour segmentation could cause a great effect on segmentation accuracy rate.

Table 1 summarizes the average sensitivity and average accuracy of breast ultrasound imaging with include contour post-processing and not include contour post-processing. The proposed contour post-processing method diminished effectively

the shadows area of tumor. Table 2 and Figures 11 show that the proposed segmentation method always identified similar contour as that obtained by EMS mode. Further work should improve execution time of the proposed segmentation algorithm, due to the VNN and region growing algorithms analyzed 3D information, the time complexity is higher than that of the 2D segmentation algorithms.

REFERENCE

[1] M. Riccabona, T. R. Nelson, and D. H. Pretorius, "Three-dimensional ultrasound: Accuracy of distance and volume measures," *Ultrasound in Obstetrics and Gynecology*, vol. 7, no. 6, pp. 429-434, June1996.

[2] D. R. Chen, R. F. Chang, W. J. Wu, W. K. Moon, and W. L. Wu, "3-D breast ultrasound segmentation using active contour model," *Ultrasound in Medicine and Biology*, vol. 29, no. 7, pp. 1017-1026, July2003.

[3] Y. H. Hsiao, Y. L. Huang, S. J. Kuo, W. M. Liang, S. T. Chen, and D. R. Chen, "Characterization of benign and malignant solid breast masses in harmonic 3D power Doppler imaging," *European Journal of Radiology*, vol. 71, no. 1, pp. 89-95, July2009.

[4] A. Madabhushi and D. N. Metaxas, "Combining low-, high-level and empirical domain knowledge for automated segmentation of ultrasonic breast lesions," *IEEE Transactions on Medical Imaging*, vol. 22, no. 2, pp. 155-169, Feb.2003.

[5] M.Cvancarova, F.Albregtsen, K.Brabrand, and E.Samset, "Segmentation of ultrasound images of liver tumors applying snake algorithms and GVF," *International Congress Series*, vol. 1281, pp. 218-223, May2005.

[6] Y. L. Huang, Y. R. Jiang, D. R. Chen, and W. K. Moon, "Level set contouring for breast tumor in sonography," *Journal of Digital Imaging*, vol. 20, no. 3, pp. 238-247, Sept.2007.

[7] Z. Dokur and T. Olmez, "Segmentation of ultrasound images by using a hybrid neural network," *Pattern Recognition Letters*, vol. 23, no. 14, pp. 1825-1936, Dec.2002.

[8] M. N. Kurnaz, Z. Dokur, and T. Olmez, "An incremental neural network for tissue segmentation in ultrasound images," *Computer Methods and Programs in Biomedicine*, vol. 85, no. 3, pp. 187-195, Mar.2007.

[9] Z. Dokur, "A unified framework for image compression and segmentation by using an incremental neural network," *Expert Systems with Applications*, vol. 34, no. 1, pp. 611-619, Jan.2008.

[10] S.Sherebrin, A.Fenster, R.N.Rankin, and D.Spence, "Freehand three-dimensional ultrasound: implementation and applications," *Physics of Medical Imaging*, vol. 2708, pp. 296-303, Feb.1996.

[11] R. N. Rohling, A. H. Gee, and L. H. Berman, "A comparison of freehand three-dimensional ultrasound reconstruction techniques," *Medical Image Analysis*, vol. 3, no. 4, pp. 339-359, Nov.1999.

[12] E. Ercelebi and S. Koc, "Lifting-based wavelet domain adaptive Wiener filter for image enhancement," *IEE Proceedings-Vision Image and Signal Processing*, vol. 153, no. 1, pp. 31-36, Feb.2006.

[13] M. I. Sezan, A. M. Tekalp, and R. Schaetzing, "Automatic Anatomically Selective Image-Enhancement in Digital Chest Radiography," *IEEE Transactions on Medical Imaging*, vol. 8, no. 2, pp. 154-162, June1989.

[14] A. Polesel, G. Ramponi, and V. J. Mathews, "Image enhancement via adaptive unsharp masking," *IEEE Transactions on Image Processing*, vol. 9, no. 3, pp. 505-510, Mar.2000.

[15] N. J. Raine-Fenning, J. S. Clewes, N. R. Kendall, A. K. Bunkheila, B. K. Campbell, and I. R. Johnson, "The interobserver reliability and validity of volume calculation from three-dimensional ultrasound datasets in the in vitro setting," *Ultrasound in Obstetrics & Gynecology*, vol. 21, no. 3, pp. 283-291, Mar.2003.

[16] N. Raine-Fenning, B. Campbell, J. Collier, M. Brincat, and I. Johnson, "The reproducibility of endometrial volume acquisition and measurement with the VOCAL-imaging program," *Ultrasound in Obstetrics & Gynecology*, vol. 19, no. 1, pp. 69-75, Jan.2002.

[17] A. Bordes, A. M. Bory, M. Benchaib, R. C. Rudigoz, and B. Salle, "Reproducibility of transvaginal three-dimensional endometrial volume measurements with virtual organ computer-aided analysis (VOCAL) during ovarian stimulation," *Ultrasound in Obstetrics & Gynecology*, vol. 19, no. 1, pp. 76-80, Jan.2002.

[18] D. CohenOr and A. Kaufman, "3D line voxelization and connectivity control," *IEEE Computer Graphics and Applications*, vol. 17, no. 6, pp. 80-87, Nov.1997.

[19] L. Pothuaud, P. Porion, E. Lespessailles, C. L. Benhamou, and P. Levitz, "A new method for three-dimensional skeleton graph analysis of porous media: application to trabecular bone microarchitecture," *Journal of Microscopy-Oxford*, vol. 199, pp. 149-161, Aug.2000.

[20] D. R. Chen, R. F. Chang, W. M. Chen, and W. K. Moon, "Computer-aided diagnosis for 3-dimensional breast ultrasonography," *Archives of Surgery*, vol. 138, no. 3, pp. 296-302, Mar.2003.

[21] P. Anbeek, K. L. Vincken, M. J. P. van Osch, R. H. C. Bisschops, and J. van der Grond, "Probabilistic segmentation of white lesions in MR imaging," *Neuroimage*, vol. 21, no. 3, pp. 1037-1044, Mar.2004.